

Your brain on bikes: P3, MMN/N2b, and baseline noise while pedalling a stationary bike

Joanna E. M. Scanlon^a, Alex J. Sieben^a, Kevin R. Holyk^a, Kyle E. Mathewson^{a,b}

^a *Department of Psychology, Faculty of Science, University of Alberta*

^b *Neuroscience and Mental Health Institute, Faculty of Medicine and Dentistry,
University of Alberta*

Corresponding Author:

Kyle E. Mathewson, Ph.D.
Department of Psychology
P-217 Biological Sciences Building
University of Alberta,
Edmonton, AB, Canada, T6G 2E9
kyle.mathewson@ualberta.ca

Abstract

Increasingly there is a trend to measure brain activity in more ecologically realistic scenarios. Normally the confines of the laboratory and sedentary tasks mitigate sources of electrical noise on electroencephalography (EEG) measurement. Moving EEG outside of the lab requires understanding of the impact of complex movements and activities on traditional EEG and ERP measures. Here we recorded EEG with active electrodes while participants were either riding or sitting on a stationary bike in an electrical and sound attenuated chamber in the lab. Participants performed an auditory oddball task, pressing a button when they detected rare target tones in a series of standard frequent tones. We quantified both the levels of spectral, single-trial baseline, and ERP baseline noise, as well as classic MMN/N2b and P3 ERP components measured during both biking and sitting still. We observed slight increases in posterior high frequency noise in the spectra, and increased noise in the baseline period during biking. However, morphologically and topographically similar MMN/N2b and P3 components were measured reliably while both biking and sitting. A quantification of the power to reliably measure ERPs as a function of the number of trials revealed slight increases in the number of trials needed during biking to achieve the same level of power. Taken in sum our results confirm that classic ERPs can be measured reliably during biking activities in the lab. Future directions will employ these techniques outside the lab in ecologically valid situations.

Your brain on bikes: P3, MMN/N2b, and baseline noise while pedalling a stationary bike

Electrophysiological and neuroimaging research has revealed a great wealth of information about brain activity, cognition, and behaviour. However most cognitive neuroscience is confined to experiments with minimal sensory stimulation and movement, often requiring subjects to remain sitting for long periods of time and avoid movement. This is because sensations, sounds, and movement introduce noise into the signal (Schlögl et al., 1990; White and Van Cott, 2010), and this noise is what primarily determines statistical power when recording EEG and ERP data (Luck, 2014). For this reason, most experiments using EEG require participants to sit completely still inside a faraday cage, devoid of the natural movements of their everyday lives.

While these neuroscience methods have held strong since the beginnings of electrophysiological recordings, they have allowed us a limited view of typical human life, which often includes shifting through a variety of movements and types of physiological stimulation. In 2011 for example, 201785 people in Canada reported cycling in their daily commutes (Statistics Canada, 2011), meaning that these individuals were making fast, critical decisions alongside other vehicles while experiencing heightened physical exertion, visual and auditory stimuli, and constant movement. Most neurophysiological studies aim to have generalizable results however, while requiring participants to avoid all natural types of movement during brain recording to avoid creating data noise. Some studies have attempted to directly measure the way in which cognitive processes may be altered during aerobically demanding exercise such as cycling, in response to these limitations.

Mobile EEG is becoming an important method for recording brain activity, with several studies improving upon previous EEG equipment to afford mobility. De Vos and Debener (2014)

recommend that these technologies be lightweight, small, and with the ability to avoid cable motion (preferably wireless). Following this recommendation, Debener and colleagues (2015) showed that a P3 ERP component can be reliably recorded from electrodes printed in a flexible sheet and placed around the ear, using a new cEEGrid electrode array. This technology was able to illustrate known spectral differences between conditions with eyes closed and open, as well as demonstrating the P3 during an oddball task at different times of the day with high test-retest reliability. Bleichner and colleagues (2015) used a similar approach to make an EEG BCI system that could be hidden under a regular baseball cap, and obtained significant P3 modulations in a BCI spelling task. Additionally, a similar BCI speller study by De Vos and colleagues (2014) was able to show equivalent results between a wireless mobile amplifier and a wired laboratory EEG system.

In terms of movement during EEG recording, studies measuring ERP signals during physical activity have shown mixed results. Yagi and colleagues (1999) observed shorter reaction times, higher error rates, and decreased P3 latency and amplitudes during exercise, for both visual and auditory task modalities. Conversely, Grego and colleagues (2004) looked at P3 amplitude and latency changes during a 3-hour cycling exercise on an ergocycle with electromagnetic brakes. They found that P3 amplitude increased between the 1st and 2nd hour, along with an increase of P3 latency after 2 hours of exercise. Pontifex and Hillman (2007) measured ERPs during conditions of rest and cycling at 60% of the subject's maximal heart rate while performing congruent and incongruent trials of a flanker task. Exercise showed increased amplitude of P3 at frontal and lateral sites, and increased P3 and N2 latencies relative to rest. Taken together, these results are contradictory, indicating a need for more studies to explain the

ways in which movements associated with biking movement without concomitant aerobic exercise can affect cognition.

Some studies have measured brain activity during sub-aerobic forms of physical activity such as walking. Gramann and colleagues (2010) recorded brain activity to a visual oddball task during standing, slow walking, fast walking, and running (on a treadmill). This study acknowledged possible artifacts from three sources: cable sway due to head movement, and eye and neck movements compensating for said head movements. The authors used a data-driven source decomposition ICA method to separate EEG brain activity data from electrical signals due to artifact. However this method was unable to analyze data collected during running because the data noise created during running made it impossible to use ICA to properly decompose the data into components. No differences in ERPs were observed between standing, slow walking, and fast walking. Debener and colleagues (2012) found that it was possible to obtain single-trial P3 classification in both indoor and outdoor recording conditions with a high degree of classification accuracy, although they noted slightly lower single trial classification accuracy when recording outside due to increased data noise. The authors also found a significantly reduced P3 amplitude while recording outside, but could not conclude whether this was the result of higher cognitive requirement or residual data noise. Using a mobile EEG BCI system, De Vos, Gandras and Debener (2014) found no significant difference in RMS data noise or the P3 between walking around campus and sitting still during an auditory oddball task. Taken together, these studies suggest that accurate ERPs may be measured during walking. As there is currently little consensus on the effects of more vigorous types of exercise, such as running or cycling during cognitive processing, it is not yet clear whether walking's limited effects on brain

activity are due to the low level of exertion compared to other exercises, or that this type of physical activity simply has no effect on brain activity in these tasks.

Recently, several studies have measured ERPs during stationary and mobile cycling. Schmidt-Kassow and colleagues (2013) used a wired-passive electrode system during an auditory oddball paradigm in which the stimulus onset interval (SOA) was either constant or variable, while participants were either sub-aerobically pedalling or sitting still on an ergometer within the lab. The authors found that P3 amplitudes were highest when using constant SOA stimuli while pedaling, with no differences due to pedalling during variable SOA. Additionally they found that the P3 amplitudes were larger and latencies were decreased while participants were pedaling with less temporal variability. In another study using a wireless mobile EEG system with passive electrodes, Zink and colleagues (2016) used an auditory oddball paradigm, while participants were either sitting, pedalling, or cycling. No differences in P3 or RMS data noise were found between pedalling and sitting, while decreased P3 and increased RMS at outer electrode sites were observed when moving around. Altogether these studies indicate that ERPs can be successfully recorded during stationary cycling with few differences from sitting still.

In addition to ERPs, some previous studies have investigated the effects of walking and cycling on cortical oscillations. Storzer and colleagues (2016) compared the oscillatory patterns during walking and cycling tasks of comparable speed. The authors found that during cycling there were decreases in the high-beta band (23-35Hz) during initiation and execution of movements, with a subsequent increase in beta power during movement termination. In comparison, walking was associated with a consistently stronger decrease in alpha power (8-12Hz). Jain, Schindler-Ivens and Schmit (2013) measured oscillations in the motor cortex using EEG, and found significantly increased beta desynchronization over motor cortex during active

pedaling compared to passive (effortless) pedaling. Additionally, they found a negative correlation between the average EEG during active trials and composite EMG signals from areas of the leg associated with the transition between flexion and extension. These studies indicate that oscillations in brain activity can be measured in the EEG during cycling.

Physical activity causes the body to experience muscle movement, tactile and vestibular sensations, perspiration, as well as increases in blood flow, respiration, and temperature. All of these physiological factors have the potential to create noise within signals and decrease statistical power. Active amplification in the electrode itself, such as that used by active low-impedance wet electrodes, attempts to decrease data noise by minimizing the distance signals must travel before being amplified. This amplification happens before movement artifacts such as those from wire movements can be incorporated into the data, decreasing the effect of these artifacts on the data, possibly making active electrodes a good candidate for studies involving movement. Electrodes with active amplification have been shown to possibly reduce the impact of movement on measures of noise including pre-stimulus noise, signal-to-noise ratio, and EEG amplitude variance (e.g. Oliviera et al., 2016). However like most EEG hardware, Active Wet electrodes were originally manufactured to be used in quiet, enclosed spaces with individuals sitting still. Therefore, exercise equipment such as stationary bicycles introduce problems with equipment (e.g. Wire movements, insufficient wire lengths, increased blood-flow, and perspiration) that require creative solutions to make EEG recording possible. To control for the possible increases in variability and data noise caused by increased blood flow, perspiration, respiration, and temperature, the present study focuses on sub-aerobic movement on a stationary bicycle. Additionally, to control for light, sound, and visual scenery in an outdoor environment

and isolate the effects of cycling movement, the present study was conducted in a laboratory faraday cage.

To test for differences in electrodes used in mobile studies, Oliviera and colleagues (2016) compared Biosemi (active amplification) wet electrodes to Cognionics wet and dry electrodes (passive electrodes with active shielding) in an oddball task with walking and seated conditions. The Biosemi active wet electrodes showed no differences in statistical noise between walking and seated conditions, while both the passive wet and passive dry electrodes showed significant increases in pre-stimulus noise and amplitude variance across the P3 component window, as well as decreases in the signal to noise ratio. While it is possible that this study was confounded by the amplifier type and electrode cap used, there appears to be some benefit to active amplification which warrants further study. Further, Laszlo and colleagues (2014) investigated differences between active and passive electrodes using different levels of impedance and the same amplifier. The authors found that while passive electrodes are ideal in conditions of extremely low impedance ($<2k \Omega$), active amplification electrodes were ideal for all impedance levels above this point. As a major concern with movement EEG recordings is the possibility of electrode and wire movements increasing levels of impedance, this study adds to evidence that active amplification may benefit mobile EEG studies. Altogether these studies imply that mobile EEG is emerging as an effective recording method, with best results using small flexible electrodes as well as with active amplification. While the present study does not intend to present a fully mobile experiment, we will attempt to determine if laboratory quality data can be collected during stationary movement using an active wet EEG system previously used in non-movement experiments.

Currently, few studies have investigated whether it is feasible to collect accurate and statistically reliable ERP measurements during sub-aerobic cycling movement in a laboratory environment. Additionally, cycling may be well suited for EEG recording due to minimal torso and head movements compared with running and walking. The current study attempts to extend the experiment on the effects of electrode type on P3 measurement of Mathewson, Harrison, and Kizuk (2017), with comparable methodology and analysis. Each participant completed an auditory P3 task while both pedaling at a sub-aerobic rate on a stationary bicycle (*Bike*), and sitting on the bike still (*Pre* and *Post*) for 15 minutes, with ERPs recorded using active low-impedance wet electrodes. The ERP traces and topographies, baseline noise levels, power spectra, and the number of trials required to gain significance for the P3 and MMN/N2b were analyzed. Particularly, the effectiveness of the active wet electrodes in measuring ERP data during sub-aerobic movement on a stationary bicycle is of interest. Our first hypothesis is that due to increases in movement during recording, the cycling conditions will demonstrate an increased amount of single-trial and ERP noise, leading to a decrease in statistical power. The second hypothesis is that even with these effects, accurate recording of ERPs will be possible during conditions before, during, and after cycling.

Method

Participants

A total of fourteen members of the university community participated in the experiment (Mean age = 25.4; Age range = 20-50; 3 female). Participants all had normal or corrected-to-normal vision with no history of neurological problems. All participants were members or associated members of The Mathewson Lab at the University of Alberta, and the experimental procedures were approved by the internal Research Ethics Board of the University of Alberta.

Materials

Prior to the start of the experiment, participants selected one of two bicycles (2015 Kona Mahuna), differing in only frame size (17 inch or 19 inch), based on participant's height. Seat height was adjusted to a comfort level as indicated by the participant. The bicycles were equipped with a small mock-press button, fastened on the right handlebar. The bicycle was then placed within a radio frequency attenuated chamber where recording eventually took place. A Volare Home Lander magnetic/fluid resistance trainer was used to ensure the bike remained stationary and was applied to the back wheel. Resistance was kept constant for all participants at a set level of 4. A plastic travel block was applied to the front wheel to ensure the bike remained balanced during the task. Participants and bike were situated in front of a magnetic black and white fixation cross was transfixed on the wall of the chamber directly in front of the participant, 143.5 cm away. Auditory stimuli were presented using a Windows 7 PC running Matlab R2012b and the Psychophysics toolbox (Brainard, 1997), and audio was output via an Asus Xonar DSX sound card. Coincident in time with sound onset, 8-bit TTL pulses were sent to the amplifier to mark the data for ERP averaging. Figure 1A shows a picture of the general set-up involved.

INSERT FIGURE 1 ABOUT HERE

Procedure

Each participant completed the auditory oddball task in each biking condition (*Pre*, *Bike*, and *Post*). A pair of Logitech Z130 speakers played one of two different frequency tones (either 1500 or 1000 Hz; sampled at 16384 Hz; One channel; 16-ms duration; 2-ms linear ramp up and down). The volume of the speakers and sound output was kept constant for every participant at a volume 90 dB (SPL) at the speaker and was situated in a constant position 116 cm away from the participants ears, providing a sound level to the participant around 59 dB SPL (-31db SPL due to

distance). The participant's task was to cycle at a slow and relatively unvarying speed while fixating the cross on the wall. Participants were instructed to press the handlebar button with the index finger of their right hand when the rare tone was heard. Figure 1B illustrates a summary of the procedure.

In each of the three biking conditions, participants completed three blocks of 250 trials separated by a self-timed break for a total of 750 trials. Each trial had a 1/5 likelihood of being a target trial. Each trial began with a uniformly random length pre-tone interval between 500 and 1000 ms, followed by the tone onset. The next pre-target period began immediately after the tone offset, with participants responding to targets during the following pre-tone interval. These block-sets were completed three times, within three separate conditions before pedaling (*Pre*), during pedaling (*Bike*), and after pedaling (*Post*), separated by a consistent three-minute break including impedance check and correction. In the *Pre*-pedaling and *Post*-pedaling conditions, participants were instructed to sit on the bicycle while performing the auditory oddball task. In the *Bike* condition, participants were instructed to pedal slowly, at a sub-aerobic level, while performing the same oddball task.

EEG Recording

Based on Laszlo and colleagues' (2014) previous lab work comparing active and passive amplification electrodes at various levels of impedance, as well as Oliviera and colleagues' (2014) comparison of active wet, passive wet, and passive dry electrodes in a mobile task, Active Wet electrodes (BrainProducts actiCAP) were selected for the study, as they previously were found to afford cleaner and better quality signals while in less than ideal recording conditions in both studies.

Ag/AgCl pin electrodes were used and arranged in 10-20 positions (Fp2, F3, Fz, F4, T7, C3, Cz, C4, T8, P7, P3, Pz, P4, P8, and Oz). Additionally, a ground electrode, embedded in the cap at position Fpz, and two reference electrodes, clipped to the left and right ear, were used. SuperVisc electrolyte gel and mild scratching with the blunted syringe tip were used to lower impedances of all the electrodes. Gel application and aforementioned techniques continued until impedances were lowered to $< 10 \text{ k}\Omega$, measured using an impedance measurement box (BrainProducts) and until data quality appeared clean and reduced of noise. EEG was recorded online referenced an electrode clipped to the left ear, and offline the data were re-referenced to the arithmetically derived average of the left and right ear lobe electrodes.

In addition to the 15 EEG sensors, 2 reference electrodes, and the ground electrode, the vertical and horizontal bipolar electrooculogram was recorded from passive Ag/AgCl disk electrodes affixed above and below the left eye, and 1 cm lateral from the outer canthus of each eye. Electrolyte gel or sand paper tape (to abrade the skin) followed by wiping of the skin using an alcohol wipe was used to lower the impedance of these EOG electrodes based on visual inspection of the data. These bipolar channels were recorded using the AUX ports of the V-amp amplifier, using a pair of BIP2AUX converters, and a separate ground electrode affixed to the central forehead.

EEG was recorded with a V-amp 16-channel amplifier (Brain Products). Data were digitized at 500 Hz with a resolution of 24 bits. Data were filtered with an online bandpass with cutoffs of 0.1 and 30 Hz, along with a notch filter at 60 Hz. These narrow filters were used as recommended in the actiCAP Xpress manual (Brain Products, 2014). All trials took place in a dimly lit sound and radio frequency attenuated chamber shielded from electro-magnetic instruments, with copper mesh covering the window. The only electrical devices in the chamber

were an amplifier, speakers, keyboard, mouse, and monitor. The fan and lights were turned on, to allow proper ventilation and visual acuity of the fixation. The monitor runs on DC power from outside the chamber, the keyboard and mouse plugged into USB outside the chamber, and the speakers and amplifier were both powered from outside the chamber. Nothing was plugged into the internal power outlets. Any devices transmitting or receiving radio waves (i.e. cellphones) were either turned off or removed from the chamber for the duration of the experiment.

EEG Analysis

Analyses were computed using Matlab R2012b using EEGLAB (Delorme and Makeig, 2004), as well as custom scripts. The timing of the TTL pulse was marked in the recorded EEG data, and used to construct 1200-ms epochs time locked to the onset of standard and target tones, with the average voltage in the first 200-ms baseline period subtracted from the data for each electrode and trial. To remove artifacts due to amplifier blocking and other non-physiological factors, any trials in any of the conditions with a voltage difference from baseline larger than $\pm 1000 \mu\text{V}$ on any channel (including eyes) were removed from further analysis. A lenient threshold was used in order to keep as many trials as possible for the power analysis, and to allow about equal numbers of rejected trials for each movement condition. At this time, a regression based eye-movement correction procedure was used to estimate and remove artifactual variance in the EEG due to blinks as well as horizontal and vertical eye movements (Gratton, Coles, and Donchin, 1984). After identifying blinks with a template based approach, this technique computes propagation factors as regression coefficients predicting the vertical and horizontal eye channel data from the signals at each electrode. The eye channel data is then subtracted from each channel, weighted by these propagation factors, removing most variance in the EEG predicted by eye movements. On average artifact rejection left roughly equal numbers

of trials per participant in the *Bike* ($M_{targ} = 139$; $range_{targ} = 101-159$; $M_{stand} = 611$; $range_{stand} = 487-638$), *Pre* ($M_{targ} = 156$; $range_{targ} = 152-165$; $M_{stand} = 601$; $range_{stand} = 568-610$), and the *Post* conditions ($M_{targ} = 146$; $range_{targ} = 82-157$; $M_{stand} = 575$; $range_{stand} = 361-608$), from which the remaining analyses are computed. No further filtering or rejection was done on the data in order to include as many trials as possible for each of the conditions and to investigate how minor sources of non-eye related noise contribute to the power to measure ERP components during the cycling task.

Results

Raw data is depicted in Figure 2A for a representative participant at the Pz electrode location. We used two separate methods to estimate the data noise of individual trials. First, we computed an average of the frequency spectra of each EEG epoch in the Fz and Pz electrode locations. Data from each participant was randomly sampled for 545 of their artifact-removed standard and target trials. A Fast Fourier Transform was computed by symmetrically adding zeros to pad the 600 time point epochs, making a 1024 point time series for each epoch, providing .488 Hz resolution frequency bins. Because data was collected online with a 30Hz low-pass filter, we only plotted frequencies measuring up to 30-Hz. The 545 spectra from each participant were then averaged together to calculate spectra for each participant, which were then combined to form a grand average spectra, illustrated in Figure 2B for two channels. Shaded regions denote standard error of the mean across participants. Evident from the plot is an increase in high frequency oscillations (>15 Hz) at Pz during the *Bike* compared to both *Pre* ($M_{Bike-Pre\ power} = 0.09$; $SD_{power} = 0.016$; $p < .0002$) and *Post* ($M_{Bike-Post\ power} = 0.054$; $SD_{power} = 0.016$; $p < .012$) conditions, as well as marginally higher power oscillations in the *Post* condition compared to *Pre* ($M_{Post-Pre\ power} = 0.036$; $SD_{power} = 0.014$; $p < .067$). Visual inspection of the

topography of this difference during biking indicated it was posterior and likely due to muscle artifacts of the neck during biking. All conditions showed both the typical peak in the alpha frequency range between 8 and 12 Hz over posterior regions (Mathewson et al., 2011), as well as the expected 1/f frequency structure in the data.

INSERT FIGURE 2 ABOUT HERE

Single-Trial Noise

To calculate an additional estimate of the noise on single trial EEG epochs, we calculated the root mean square (RMS) of a baseline period for each trial (De Vos et al., 2014). The baseline consisted of the time period 200ms (100 time points) prior to each tone's onset, to avoid inclusion of any interference due to the evoked ERP activity in the RMS measurement. The RMS is equivalent to the average absolute voltage difference around the baseline, and is therefore a good estimate of single trial noise within EEG data. To estimate RMS distribution for each condition in our data, we used a permutation test which selects a different set of 360 epochs without replacement for each participant on each of 10,000 permutations prior to running second order statistics (Laszlo et al., 2014; Mathewson et al., 2017). A grand average single-trial RMS was computed and recorded for each of these random selections and for each condition. A histogram of the grand average single-trial RMS values calculated for each permutation is shown in Figure 2C, for each condition. Figure 2D shows a bar graph of the mean and standard deviation of grand average and single-trial RMS permutation distributions. The results show clear distinction between the single-trial noise of each condition. The *Bike* condition ($M_{RMS-EEG} = 6.815$; $SD_{RMS-EEG} = 0.031$) showed clearly larger single trial noise levels, which was reliable compared to both the *Pre* ($M_{RMS-EEG} = 5.979$; $SD_{RMS-EEG} = 0.020$; $z = 122.472$; $p < .0001$) and

Post conditions ($M_{RMS-EEG} = 6.373$; $SD_{RMS-EEG} = 0.019$; Wilcoxon rank sum test; $z = 122.472$; $p < .0001$). The *Pre* condition had lower single trial noise than the *Post* ($z = -122.472$; $p < .0001$).

ERP Baseline Analysis

Following this process, we analyzed noise levels within trial-averaged ERPs. Figure 3A plots the grand averaged ERPs for each condition, at the Pz and Fz electrode locations separated between standards and targets, in order to compare the ERPs of both standards and targets between biking conditions. Clearly during biking it is possible to measure ERPs with very similar morphology and topography to those measured while sitting still. Visual inspection of the ERP morphology compared to uncorrected eye channels revealed no discernable differences in the effectiveness of the artifact rejection procedures and removing eye related artifacts from the data. Evident from the graphs is the expected increase in amplitude for the P3 during target trials toward the back of the head (Pz), with a slightly greater P3 amplitude for targets in the *Pre*-condition.

INSERT FIGURE 3 ABOUT HERE

We again used a permutation test of the RMS values in the baseline period to quantify the amount of noise in the participant average ERPs. Complementary to the single-trial RMS analysis above, this calculation estimates the amount of phase-locked EEG noise in the data that is not averaged out over trial with respect to the tone onset. We averaged 360 standard trials, which were randomly selected without replacement from all of each participant's non-artifact trials in the standard condition. These RMS values were then averaged over EEG electrodes, allowing us to compute a grand average for all participants, creating 10,000 permutations once participant's data were averaged together to compute second order statistics. Figure 4B depicts a histogram of the RMS grand averages computed with the 10,000 permutations of each condition.

The bargraph in Figure 4C shows the means of these distributions, with error bars to indicate the standard deviation of the distribution of permutation means. While pedaling in the *Bike* condition ($M_{RMS-ERP} = 0.405$; $SD_{RMS-ERP} = 0.019$) produced a higher RMS value compared with both the *Pre* ($M_{RMS-ERP} = 0.337$; $SD_{RMS-ERP} = 0.014$; $z = 122.201$; $p < .0001$) and the *Post* conditions ($M_{RMS-ERP} = 0.360$; $SD_{RMS-ERP} = 0.011$; $z = 117.917$; $p < .0001$), *Pre*-pedaling also showed reliably smaller ERP noise compared to *Post*-pedaling ($z = -99.080$, $p < .0001$).

INSERT FIGURE 4 ABOUT HERE

ERP Morphology and Topography

Figure 4A demonstrates grand average ERPs following standard and target tones from electrode Pz, calculated only from each participant's artifact-free and corrected trials. The graphs' shaded regions depict the standard error of the mean for each time point, within each tone type. Similar levels of error were shown across all three conditions. As expected, a P3 oddball difference was demonstrated, with increased positive voltage between 300-430 ms following infrequent target tones, when compared to frequent standard tones. This time window was used for all further ERP analysis of the P3. Additionally evident in Figure 5A was a difference between stimuli in the windows of the mismatch negativity (MMN) and N2b, with a more negative voltage between 175-275 ms following the infrequent targets tones when compared to the frequent standard tones at electrode Fz. This time window was used for the majority of further ERP analysis of the MMN/N2b.

Figure 4B illustrates topographies of this difference within the P3 and MMN/N2b windows. P3 topographies reveal the expected central posterior scalp distribution of activation for all three conditions, while MMN/N2b topographies reveal the expected central anterior distribution of activation. Figure 3C shows the difference waves at Pz which subtract each

participant's standard tone ERPs from their target tone ERPs. Shaded regions in this Figure represent the within-participant standard error of the mean, because variation between-participants was attenuated due to the subtraction of standards from targets. Therefore, this error estimate is equivalent to that used in the t -test of this difference from zero (Loftus and Masson, 1994).

For all conditions, there was a clear negative peak evident at approximately 220 ms even on the posterior electrode. A one-tailed, paired-sample t -test comparing this MMN/N2b difference at electrode Fz in a window from 175-275 ms centered around this observed peak revealed a significant MMN/N2b effect for the *Bike* condition ($M_{diff} = -1.911$; $SD_{diff} = 2.077$; $t(13) = -3.441$; $p = .0022$), the *Pre* condition ($M_{diff} = -2.115$; $SD_{diff} = 1.753$; $t(13) = -4.515$; $p = .00029$), and the *Post* condition ($M_{diff} = -1.474$; $SD_{diff} = 1.902$; $t(13) = -2.900$; $p = .0062$). Further, as expected a clear positive peak at around 380 ms was observed at Pz. A one-tailed, paired-sample t -test comparing this P3 difference at electrode Pz in the window from 300-430 ms revealed a significant P3 effect for the *Bike* condition ($M_{diff} = 3.321$; $SD_{diff} = 2.362$; $t(13) = 5.260$; $p = .000077$), the *Pre* condition ($M_{diff} = 4.170$; $SD_{diff} = 3.493$; $t(13) = 4.467$; $p = .00032$), and the *Post* condition ($M_{diff} = 3.054$; $SD_{diff} = 2.766$; $t(13) = 4.131$; $p = .00059$).

ERP Power

Figure 5A plots difference waves for each of the three biking conditions for electrode locations Fz and Pz. As shown, there are no significant differences of the MMN/N2b between conditions at Fz. A repeated measures ANOVA test across the three biking conditions showed no main effect of biking condition on the MMN/N2b amplitude ($F(2,13) = 1.704$, $p = .202$). In order to understand differential contribution to this effect of the MMN and N2b, we also separated this window and differentially analyzed an early MMN time period (100-200 ms) and a later N2b

time period (200-300 ms) to look for differential effects on these two components. No significant differences in the target minus standard data between conditions were found in a repeated measures ANOVA applied to either the MMN window (at Fz: $F(2,13) = 0.2$; $p = .82$; at Pz: $F(2,13) = 0.975$; $p = 0.3905$), or the later N2b window (at Fz: $F(2,13) = 2.165$; $p = .1350$; at Pz: $F(2,13) = 0.614$, $p = 0.5487$). Both the MMN and N2b were likely elicited here, however with the current design it is not possible to disentangle them from each other, while it is also beyond the scope of the current study to do so. From here on we therefore focus on the combined MMN/N2b window between 175 and 275 ms.

INSERT FIGURE 5 ABOUT HERE

For the P3, a repeated measures ANOVA test across the three biking conditions revealed only a marginal main effect of biking condition on P3 amplitude ($F(2,13) = 2.700$, $p = .0860$). Simple effects tests showed that while the P3 amplitude at Pz in the *Bike* condition did not reliably differ from either the *Pre* ($t(13) = 1.588$, $p = .136$) or *Post* condition ($t(13) = 0.628$, $p = .541$), there was a marginal decrease in P3 amplitude from *Pre* to *Post* biking ($t(13) = 2.077$; $p = 0.0582$). Figure 5B shows the corresponding topographies to these differences for the MMN/N2b and the P3.

Following evidence for increased trial-averaged and single-trial noise in the *Bike* condition when compared to the *Pre* and *Post* conditions, one might expect to observe a lower statistical power in the *Bike* condition. To explicitly test this prediction, we used a permutation procedure in which we kept the 4:1 ratio of standard to target trials constant while varying the number of trials contributing to the ERP average. Trial numbers increased from 4 standards and 1 target trial, by 20 standard trials, up to 300 standards and 75 target trials. We then randomly selected with replacement this number of trials from each participants overall trials, then

averaged over subjects to get second order statistics (grand averages). This random replacement was done separately for each biking condition, and for both the MMN/N2b and P3 analyses. For each number of trials, 10,000 permutations of this procedure were done. Note that this procedure does not consider possible changes in ERP magnitude or morphology over time in the task due to attention or habituation, and assumes that these influences are constant across conditions and stimuli.

For each permutation, the single trials selected were averaged to create separate participant ERPs for target and standard tones. The difference between standard and target tones was then calculated at electrode Pz between 300 and 430 ms, and at electrode Fz between 175 and 275 ms in order to measure the P3 and MMN/N2b average values, respectively. These participant average ERP differences were then compared using a paired-sample t-test ($df = 13$, one-tailed, $\alpha = .05$). Figure 5C plots the proportion out of 10,000 permutations in which the t-statistic obtained passed the significance threshold, as a function of the number of samples selected for each permutation. It is evident from this graph that the MMN/N2b from the *Pre* condition reached significance on 80% permutations (80% power grey line) with less trials (20 target/80 standard trials) than did the *Post* condition (60 target/240 standard trials), with the *Bike* condition lying between these (35 target/140 standard trials). The effect is similar in the P3: the *Pre*-cycling condition required 10 targets/40 standards, the *Bike* condition requires 10 targets/40 standards, and the *Post* condition requires 15 targets/60 standards to reach an 80% level of power.

Discussion

The present study directly examined the effectiveness of measuring ERPs while cycling on a stationary bicycle, compared with data collected while sitting still before and after cycling.

The results supplement findings from some other studies of mobile EEG that movement increases mechanical artifacts and single trial noise (e.g. Gramann et al., 2010; but see De Vos et al., 2014). In fact, here statistical power appeared to be more highly affected by the amount of time spent on task than data noise per se. A visual inspection of the raw data, as well as single-trial RMS and single-trial EEG spectra values showed a greater amount of data noise present during the cycling condition, even with the reduction of noise allowed by active amplification electrodes (Mathewson, et al., 2017; Oliviera et al., 2016). It is possible that some of this motion changed the electrode connections, and therefore impedance, leading to the changes observed in the Post-cycling condition, but note that we checked impedance values (ensuring $< 10 \text{ k}\Omega$ impedance levels) before each block. However in spite of this increase in data noise, typical ERP patterns were found within all conditions, illustrating that while active wet electrodes are sensitive to movement, accurate ERP measurement during mobile activity is possible.

All conditions including the cycling condition showed a reliable $1/f$ EEG spectra, with the expected alpha peak in the 7-12 Hz range at Pz (Figure 2B; Mathewson et al., 2011). However we note an increase in high frequency power in the cycling condition at Pz, believed to be due to the detection of high frequency vibrations caused by movement of the head, neck muscles, or electrode wires. Increased baseline and ERP noise is also apparent in Figures 2C, 2D, 3B and 3C, which is also believed to be due to mechanical movement caused by cycling. This noise may be more apparent because we did not use additional filtering (outside of the standard ERP filtering used inside the lab) to remove movement artifacts in this study. While this practice allowed us to investigate the movement artifacts created during cycling, future studies for cognitive experimental purposes, as well as those involving more vigorous movement such as running may require additional filtering to more accurately measure ERPs, similar to the

algorithm used by Gwin, Gramann, Makeig, and Ferris (2010). As well, these results must be interpreted with respect to the narrow passband (cutoffs of 0.1 and 30 Hz), used in accordance with recommendations in the actiCap Xpress manual (Brain Products, 2014). This narrow passband may have limited our ability to observe slow moving components in the data.

In spite of this increase in noise, however, the ERPs plotted in Figure 3A demonstrate that active wet electrodes allowed us to record laboratory-quality ERP waveforms and scalp topographies during cycling. Similar to Gramann and colleagues (2010), Debener and colleagues (2012), and De Vos, Gandras and Debener (2014), we were able to reveal reliable P3 differences between standard and target tones over posterior-central scalp locations with an approximate latency during both cycling and sitting still. This topography and timing was highly similar to those recorded in the pre-cycling and post-cycling conditions. As well, as shown in Figure 3C, the cycling movement did not show any obvious increases in size of the error bars of the ERP waveforms, even though no differences in filtering were used between conditions. Because we did not predict any cognitive effects at this low speed of biking, here we did not measure response times or accuracy in the task, which we are currently doing in follow up studies outside on the bike.

ERP differences

We also investigated qualities of the ERP components recorded. Due to the dual-task nature of the cycling condition, and because it has been shown that the P3 to target stimuli tends to decrease while performing a secondary task due to reduced cognitive resources (Polich and Kok et al., 1995; Kramer and Strayer, 1988; Polich, 1987b; Wickens, Kramer, Vanasse and Donchin, 1983) it might be expected that the P3 would be reduced during the cycling condition. However, as shown in Figure 5A, no significant differences were found between the conditions

at the Pz electrode location during biking. This is similar to the lack of P3 difference between walking and standing (Gramann and colleagues, 2010) or sitting (De Vos, Gandras and Debener, 2014) found in previous studies and may be due to the low task-load involved with cycling, as the activity does not require a great deal of focus, especially when stationary. The findings also echo those of Zink and colleagues and (2016) Schmidt-Kassow and colleagues (2013) who did not find any P3 effect for pedaling compared to sitting in a variable SOA oddball paradigm similar to ours. Here, a surprising reduction in P3 from pre- to post-exercise was observed, with the post condition showing a marginally reduced P3 compared to the pre-cycling condition. Given that the two conditions are identical and differ only in the length of time participants had been performing the task, this effect may be explained by habituation effects to the task itself, as the P3 has been shown to dissipate over time as a task becomes less novel, particularly at frontal locations (Wintink, Segalowitz, & Cudmore, 2001; Lew & Polich, 1993). However, as the task was relatively simple and confounds rarity, physical feature difference, and task relevance for the deviating stimulus, it may be that only one subcomponent of the P3a and P3b complex is modulated and we were unable to isolate these contributions. This marginal effect warrants future study, and the effect of habituation could be teased apart by counterbalancing biking and rest conditions in future studies. For example, another study currently in preparation had participants performing the same oddball task while both sitting inside and cycling outside, with an equal number of participants starting in each condition to account for habituation effects (Scanlon et al., in preparation).

Statistical Power

To investigate the number of trials required to maximize statistical power in each condition, we utilized an analysis process similar to those used by Kappenman and Luck (2010),

Laszlo and colleagues (2014), and Mathewson and colleagues (2017). In this procedure we resampled trials in order to estimate the number of trials required to demonstrate a certain amount of statistical power. This procedure shows results proportional to the signal-to-noise level of the data, and can be used to estimate the approximate number of trials needed to reliably determine a statistical effect when one exists. The results in Figure 5C showed that the pre-cycling condition required the least amount of trials for statistical reliability in both the P3 and MMN/N2b, confirming previous findings that stationary recording environments are best for achieving statistical power in an EEG study (Debener et al., 2012; Gramann et al., 2010). However while we would expect the trials during the cycling condition to have the least statistical power due to their increased noise, in fact the post-cycling condition required the greatest number of trials to obtain 80% statistical reliability. This decrease in power post-cycling may be due to habituation effects on the P3, or due to the stimuli being allocated less attentional resources after an extended period of time performing the task. These effects have been previously shown for the P3 (Polich and Kok et al., 1995; Kramer, Schneider, Fisk and Donchin, 1986; Polich, 1989a; Siddle, 1991) as well as for the MMN/N2b (Sams, Alho, & Näätänen, 1984; Näätänen, 1992). These effects may also be driven by excessive noise within individual subjects on a subset of their trials. This again suggests the need for multiple biking conditions interspersed with rest conditions in future counterbalanced designs.

Another factor to consider in the power analysis is possible increases in sensor-skin impedance. As the cycling task included recording during movement for a significant period of time, an alternate explanation for the decrease in power of the *Post* condition could be deterioration in signal quality due to these movements. However to avoid this possibility, electrode impedance levels were tested between conditions, and adjusted to ensure that

impedance levels were always below 10 k Ω . Additionally if increases in sensor-skin impedance were having a significant effect we might also expect a similar deterioration, to a lesser extent, in the bike condition. While we did observe a decrease in power of the cycling condition, this is no more of a decrease in power than would be expected for the increases in RMS data noise observed during the cycling condition. Therefore we believe that the power decreases in the *Post* condition are best explained by task-time habituation effects.

Future Directions

As we begin to use these novel EEG technologies outside of the lab, similar methods will be utilized to test the statistical power of ERP and EEG recordings in these novel environments. The present study recorded electrophysiological data inside a radio frequency shielded chamber which reduces sound and electromagnetic fields in the recording environment, however research-quality data has been shown to be recorded without radio frequency shielding (Debener et al., 2012; De Vos, Gandras, and Debener, 2014). Further research is needed to investigate the levels of noise created when Active Wet electrodes are taken outside of this controlled environment. In addition to this, the use of active amplification electrodes in mobile conditions warrants further study, as a fully conclusive comparison has yet to be made between active and passive electrodes during motion and mobile conditions. Our lab intends to perform future work in which we compare active and passive amplification electrodes with otherwise identical set-up (e.g. using the same amplifier, electrode configuration, etc.) during mobile conditions.

Currently in our lab, work is underway to begin testing these same ERP and EEG recording measures using similar tasks and while performing physical activities such as standing, walking, cycling (Scanlon et al., in preparation), and driving. These studies will utilize novel portable technologies for stimulus presentation (Kuziek, Shienh, and Mathewson, 2017). We will

deal with the expected increases in noise due to movement by continuing to use active wet electrodes, using a larger number of trials, employing additional filtering when needed, and counterbalancing of conditions.

Conclusions

In summary, we have shown that using the active EEG electrodes it is possible to accurately record and measure ERP data while individuals are biking on a stationary bike. We observed that despite the increases in data noise that mechanical movement induced with cycling, it is possible to measure ERPs without any extensive filtering procedures. We also observed that after recording for long periods of time, habituation effects begin to take place, causing the last set of trials to show reduced ERPs and decreased statistical power. Increased numbers of trials were required to achieve the same probability of showing a significant standard-target difference when one was present. However, using a traditional ERP task we were nonetheless able to measure ERP and EEG signatures reliably during consistent mechanical movement. This study therefore provided an estimate of our ability to measure ERPs during cycling movement, which serves as an important step for the community to begin to utilize mobile EEG techniques and bring cognitive neuroscience into the real world.

References

- Brain Products GmbH. Brain Products actiCAP Xpress – much more than just a dry electrode system. [Brochure]. Munich, Germany; 2014. Retrieved April 20, 2015 from <http://pressrelease.brainproducts.com/brain-products-acticap-xpress-much-more-than-just-a-dry-electrode-system/>
- Bleichner, M. G., Lundbeck, M., Selisky, M., Minow, F., Jäger, M., Emkes, R., ... & De Vos, M. (2015). Exploring miniaturized EEG electrodes for brain-computer interfaces. An EEG you do not see? *Physiological Reports*, 3(4), e12362. doi: 10.14814/phy2.12362.
- Brainard, D. H. (1997). The psychophysics toolbox. *Spatial Vision*, 10, 630 433–436. doi: 10.1163/156856897X00357.
- Cotman, C. W., Berchtold, N. C., & Christie, L. A. (2007). Exercise builds brain health: key roles of growth factor cascades and inflammation. *Trends in Neurosciences*, 30(9), 464–472. doi: 10.1016/j.tins.2007.06.011.
- Debener, S., Minow, F., Emkes, R., Gandras, K., de Vos, M., 2012. How about taking a low-cost, small, and wireless EEG for a walk? *Psychophysiology*, 49 (11), 1449–1453. doi: 10.1111/j.1469-8986.2012.01471.x.
- Debener, S., Emkes, R., De Vos, M., & Bleichner, M. (2015). Unobtrusive ambulatory EEG using a smartphone and flexible printed electrodes around the ear. *Scientific Reports*, 5. doi: 10.1038/srep16743.
- De Vos, M., & Debener, S. (2014). Mobile EEG: towards brain activity monitoring during natural action and cognition. *International Journal of Psychophysiology*, 91(1), 1-2. doi: 10.1016/j.ijpsycho.2013.10.008.

- De Vos, M., Gandras, K., & Debener, S. (2014). Towards a truly mobile auditory brain-computer interface: Exploring the P300 to take away. *International Journal of Psychophysiology*, *91*(1), 46-53. doi: 10.1016/j.ijpsycho.2013.08.010.
- De Vos, M., Kroesen, M., Emkes, R., & Debener, S. (2014). P300 speller BCI with a mobile EEG system: comparison to a traditional amplifier. *Journal of Neural Engineering*, *11*(3), 036008. doi: 10.1088/1741-2560/11/3/036008.
- De Waard, D. (1996). The measurement of drivers' mental workload. *Groningen University, Traffic Research Center*. doi: 10.1007/978-1-4757-0884-4_23.
- Geisler, M.W., & Squires, N.K. (1992). Exercise and pain differentially affect the P300 event-related brain potential (abstract). *Psychophysiology*, *29*, S14. doi: 10.1111/j.1469-8986.2004.symp_11.x.
- Gramann, K., Gwin, J. T., Bigdely-Shamlo, N., Ferris, D. P., & Makeig, S. (2010). Visual evoked responses during standing and walking. *Frontiers in Human Neuroscience*, *4*, 202. doi: 10.3389/fnhum.2010.00202.
- Grego, F., Vallier, J. M., Collardeau, M., Bermon, S., Ferrari, P., Candito, M., ... & Brisswalter, J. (2004). Effects of long duration exercise on cognitive function, blood glucose, and counterregulatory hormones in male cyclists. *Neuroscience Letters*, *364*(2), 76-80. doi: 10.1016/j.neulet.2004.03.085.
- Gwin, J. T., Gramann, K., Makeig, S., & Ferris, D. P. (2010). Removal of movement artifact from high-density EEG recorded during walking and running. *Journal of Neurophysiology*, *103*(6), 3526-3534. doi: 10.1152/jn.00105.2010.

- Hillman, C. H., Castelli, D. M., & Buck, S. M. (2005). Aerobic fitness and neurocognitive function in healthy preadolescent children. *Medicine and Science in Sports and Exercise*, 37(11), 1967. doi: 10.1249/01.mss.0000176680.79702.ce.
- Hillman, C. H., Erickson, K. I., & Kramer, A. F. (2008). Be smart, exercise your heart: exercise effects on brain and cognition. *Nature Reviews Neuroscience*, 9(1), 58-65. doi: 10.1038/nrn2298.
- Hruby, T., Marsalek P. (2003). Event-related potentials – the P3 wave. *Acta Neurobiologiae Experimentalis*, 63, 55–63. doi: 10.1075/ce.4.1.05bal.
- Jain, S., Gourab, K., Schindler-Ivens, S., & Schmit, B. D. (2013). EEG during pedaling: evidence for cortical control of locomotor tasks. *Clinical Neurophysiology*, 124(2), 379-390. doi: 10.1016/j.clinph.2012.08.021.
- Janssen, W.H. & Gaillard, A.W.K. (1985). EEG and heart rate correlates of task load in car driving. In A. Gundel (Ed.), *Proceedings of the workshop 'Electroencephalography in transport operations'*. Köln, Germany: DFVLR-Institut für Flugmedizin. doi: 10.1016/0013-4694(85)90093-8.
- Kramer, A.F., Schneider, W., Fisk, A., & Donchin, E. (1986). The effects of practice and task structure on components of the event-related potential. *Psychophysiology*, 23, 33-42. doi: 10.1111/j.1469-8986.1986.tb00590.x.
- Kramer, A.F., & Strayer, D.L. (1988). Assessing the development of automatic processing: an application of dual-track and event-related brain potential methodologies. *Biological Psychology*, 26, 231-267. doi: 10.1016/0301-0511(88)90022-1.

- Kumar, N., Singh, M., & Sood, S. (2012). Effect of acute moderate exercise on cognitive P300 in persons having sedentary lifestyles. *International Journal of Applied and Basic Medical Research*, 2(1), 67. doi: 10.4103/2229-516x.96813.
- Kuziek, J. W., Shienh, A., & Mathewson, K. E. (2017). Transitioning EEG experiments away from the laboratory using a Raspberry Pi 2. *Journal of Neuroscience Methods*, 277, 75-82. doi: 10.1016/j.jneumeth.2016.11.013.
- Laszlo, S., Ruiz-Blondet, M., Khalifian, N., Chu, F., & Jin, Z. (2014). A direct comparison of active and passive amplification electrodes in the same amplifier system. *Journal of Neuroscience Methods*, 235, 298-307. doi: 10.1016/j.jneumeth.2014.05.012.
- Lew, & Polich, J. (1993). P300, habituation, and response mode. *Physiology and Behavior*, 53, 111- 117. doi: 10.1016/0031-9384(93)90018-b.
- Loftus, G. R., & Masson, M. E. (1994). Using confidence intervals in within-subject designs. *Psychonomic Bulletin & Review*, 1, 476–490. doi: 10.3758/bf03210951.
- Luck, S. J. (2014). *An introduction to the event-related potential technique*. MIT press. doi: 10.1086/506120.
- Magnie, M. N., Bermon, S., Martin, F., Madany-Lounis, M., Suisse, G., Muhammad, W., & Dolisi, C. (2000). P300, N400, aerobic fitness, and maximal aerobic exercise. *Psychophysiology*, 37(03), 369-377. doi: 10.1111/1469-8986.3730369.
- Mathewson, K. E., Harrison, T. J., & Kizuk, S. A. (2017). High and dry? Comparing active dry EEG electrodes to active and passive wet electrodes. *Psychophysiology*, 54(1), 74-82. doi: 10.1111/psyp.12536.

- Mathewson, K. E., Lleras, A., Beck, D. M., Fabiani, M., Ro, T., & Gratton, G. (2011). Pulsed out of awareness: EEG alpha oscillations represent a pulsed-inhibition of ongoing cortical processing. *Frontiers in Psychology, 2*. doi: 10.3389/fpsyg.2011.00099.
- Näätänen, R. (1992). The mismatch negativity. *Attention and Brain Function, 136-200*. doi: 10.1037/e516062012-002.
- Oliveira, A. S., Schlink, B. R., Hairston, W. D., König, P., & Ferris, D. P. (2016). Proposing Metrics for Benchmarking Novel EEG Technologies Towards Real-World Measurements. *Frontiers in Human Neuroscience, 10*. doi: 10.3389/fnhum.2016.00188.
- Polich, J., & Kok, A. (1995). Cognitive and biological determinants of P300: an integrative review. *Biological Psychology, 41(2)*, 103-146. doi: 10.1016/0301-0511(95)05130-9.
- Polich, J., & Lardon, M. T. (1997). P300 and long-term physical exercise. *Electroencephalography and Clinical Neurophysiology, 103(4)*, 493-498. doi: 10.1016/s0013-4694(97)96033-8
- Polich, J. (1987a). Response mode and P300 from auditory stimuli. *Biological Psychology, 25*, 61-71. doi: 10.1016/0301-0511(87)90067-6.
- Polich, J. (1989a). P300 habituation from auditory stimuli. *Psychobiology, 17*, 19-28. doi: 10.1016/0301-0511(87)90067-6.
- Pontifex, M. B., & Hillman, C. H. (2007). Neuroelectric and behavioral indices of interference control during acute cycling. *Clinical Neurophysiology, 118(3)*, 570-580. doi: 10.1016/j.clinph.2006.09.029.
- Sams, M., Alho, K., & Näätänen, R. (1984). Short-Term Habituation and Dishabituation of the Mismatch Negativity of the ERP. *Psychophysiology, 21(4)*, 434-441. doi: 10.1111/j.1469-8986.1984.tb00223.x.

- Scanlon, J.E.M., Townsend, K.A., Cormier, D.L., Kuziek, J.W.P., & Mathewson, K.E. (*in preparation*). Taking off the training wheels: Measuring auditory P300 during outdoor cycling.
- Schlögl, A., Anderer, P., Roberts, S. J., Pegenzer, M., & Pfurtscheller, G. (1999, November). Artefact detection in sleep EEG by the use of Kalman filtering. *In Proc. EMBEC* (Vol. 99, pp. 1648-1649). doi: 10.1016/b978-044450270-4/50025-5.
- Siddle, D.A. (1991). Orienting, habituation and resource allocation: an associative analysis. *Psychophysiology*, 28, 245-259. doi: 10.1111/j.1469-8986.1991.tb02190.x.
- Statistics Canada. (2011). Commuting to work. *Statistics Canada Catalogue no. 12-591-X*. /pub/12-591-x/12-591-x2009001-eng.htm (accessed June 13, 2015).
- Storzer, L., Butz, M., Hirschmann, J., Abbasi, O., Gratkowski, M., Saupe, D., ... & Dalal, S. S. (2016). Bicycling and walking are associated with different cortical oscillatory dynamics. *Frontiers in Human Neuroscience*, 10. doi: 10.3389/fnhum.2016.00061.
- Tomporowski, P. D., & Ellis, N. R. (1986). Effects of exercise on cognitive processes: A review. *Psychological Bulletin*, 99(3), 338. doi: 10.1037//0033-2909.99.3.338.
- van Praag, H. (2009). Exercise and the brain: something to chew on. *Trends in Neurosciences*, 32(5), 283-290. doi: 10.1016/j.tins.2008.12.007.
- White, D. M., & Van Cott, C. A. (2010). EEG artifacts in the intensive care unit setting. *American Journal of Electroneurodiagnostic Technology*, 50(1), 8-25. doi: 10.1080/1086508x.2010.11079750.
- Wicken, C., Kramer, A., Vanesse, L., & Donchin, E. (1983). The performance of concurrent tasks: a psychophysiological analysis of the reciprocity of information processing resources. *Science*, 221, 1080-1082. doi: 10.1126/science.6879207.

Wintink, A. J., Segalowitz, S. J., & Cudmore, L. J. (2001). Task complexity and habituation effects on frontal P300 topography. *Brain and Cognition*, *46*(1), 307-311. doi:

10.1016/s0278-2626(01)80090-7.

Yagi, Y., Coburn, K. L., Estes, K. M., & Arruda, J. E. (1999). Effects of aerobic exercise and gender on visual and auditory P300, reaction time, and accuracy. *European Journal of Applied Physiology and Occupational Physiology*, *80*(5), 402-408. doi:

10.1007/s004210050611.

Author Notes

The authors declare no competing financial interests. This work was supported by a NSERC discovery grant and startup funds from the Faculty of Science of KEM. The authors would like to thank Sayeed Kizuk for assistance with data collection. Reprints: Kyle E. Mathewson (kyle.mathewson@ualberta.ca)

Figure Captions

Figure 1. Stationary biking EEG apparatus and procedure. A: During the whole of the experiment, participants were seated on a stationary bike wearing an EEG cap. B: The procedure involved three conditions: *Pre*, *Bike*, and *Post*. Within each condition, participants performed the auditory oddball task for three blocks of 250 trials, separated by self-paced breaks. The standard tones played at 500Hz, while the rare tones played at 1000Hz with a 0.5-1sec interval at a ratio of 1:4 target standard trials.

Figure 2. Single trial data noise levels. A: Raw EEG data (with notch filters and online bandpass) for a representative subject for several minutes in each of the pedaling conditions, shown at the Pz electrode location. B: Single-trial EEG spectra from electrodes Fz and Pz, computed with FFTs padded with zeros on 545 auditory target trial epochs of each subject, averaged over trials first, then subjects. Shaded regions indicate the standard error of the mean. C: Histogram of root mean square (RMS) grand average values collected during a 200ms baseline period, for 10,000 permutations of 300 randomly chosen standard target trials for each subject. RMS values are averaged over all electrodes within each trial, then averaged over trials, then subjects. D: Bar graph of these permuted distributions, with error bars representing standard deviation of the permuted distributions.

Figure 3. Baseline ERP noise. A: Grand average ERPs for the Fz and Pz electrodes, plotted separately to compare standards and targets between cycling conditions. Shaded areas represent the standard error of the mean. B: Histogram of ERP baseline RMS values, calculated using 10,000 randomly selected permutations of 300 target and standard trials for each subject. For each permutation, RMS of the baseline period is computed and the

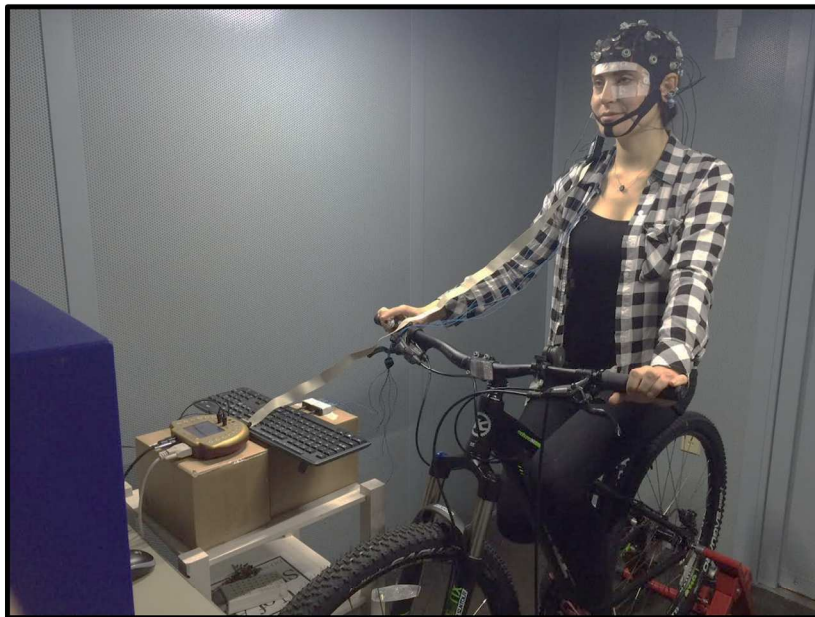
data are averaged over trials. C: Bar graph of these permuted distributions, with error bars representing standard deviation of the permuted distributions.

Figure 4. Event-related potential (ERP) grand averages. A: Grand average ERPs computed at electrode Pz for all artifact-free trials, corrected for eye movements, for both standard (black) and target (colour) tones. Positive is plotted down and shaded areas illustrate the standard error of the mean. B: Scalp topographies of the grand average ERP difference between standard and target tones in the MMN/N2b and P3 time-windows (indicated in yellow in 3C), 175-275ms and 300-430ms after the tone, respectively. EEG was re-referenced to the average of the left and right ear lobe electrodes. C: Difference wave ERPs from electrode Pz for each of the pedaling conditions, with shaded regions depicting within-subject standard error of the mean for this difference, having removed between-subject differences (Loftus and Masson, 1994). Regions highlighted in yellow depict the time-window for MMN/N2b and P3 analysis as well as topographic plotting.

Figure 5. Difference waves and ERP power analysis. A: Difference waves depicting the average difference between standard and target trials for the three biking conditions are plotted for the Fz and Pz electrode locations. Yellow highlighted regions indicate the main time windows compared, namely the MMN/N2b at Fz (left) and the P3 at Pz (right). B: Topographies illustrating the voltage difference between conditions in the comparisons of the MMN/N2b at Fz and P3 at Pz (indicated in yellow regions of 5A) C: The results of a test of permutations in which a number of trials selected within 10,000 permutations varied between 5 and 280, while keeping the 4:1 ratio of standards to targets. Randomly selected trials are averaged to compute subject ERPs with each permutation for each number of trials. Before grand average statistics are computed, differences in the P3 and MMN/N2b

time window between target and standard trials is calculated, and compared using an across subjects (paired-sample) one-tailed t -test ($\alpha = .05$). The graph plots the proportions of the 10,000 permutations for each number of trials in which an uncorrected significant difference obtained, for each of the cycling conditions. The dashed horizontal line at 0.8 represents the threshold to achieve 80% power to find an effect when one exists. The grey line shows a square root of the number of standard trials, scaled to a range between 0 and 1 on the vertical axis by dividing by the square root of the maximum number of trials.

A



B

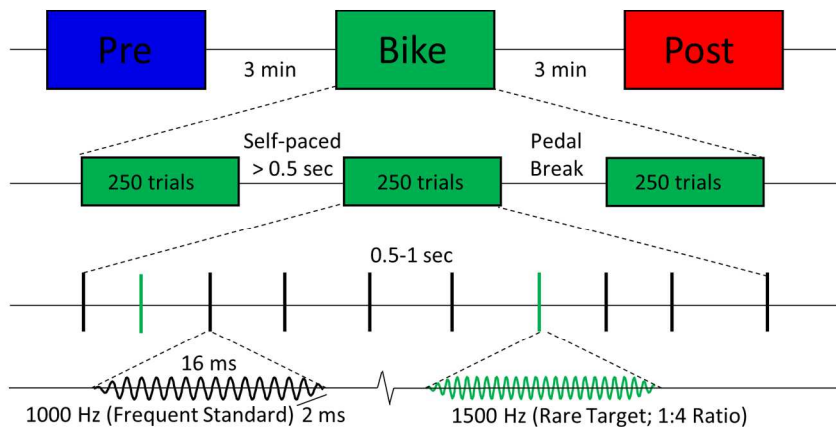


Figure 1. Stationary biking EEG apparatus and procedure. A: During the whole of the experiment, participants were seated on a stationary bike wearing an EEG cap. B: The procedure involved three conditions: Pre, Bike, and Post. Within each condition, participants performed the auditory oddball task for three blocks of 250 trials, separated by self-paced breaks. The standard tones played at 500Hz, while the rare tones played at 1000Hz with a 0.5-1sec interval at a ratio of 1:4 target standard trials.

Figure 1
145x185mm (300 x 300 DPI)

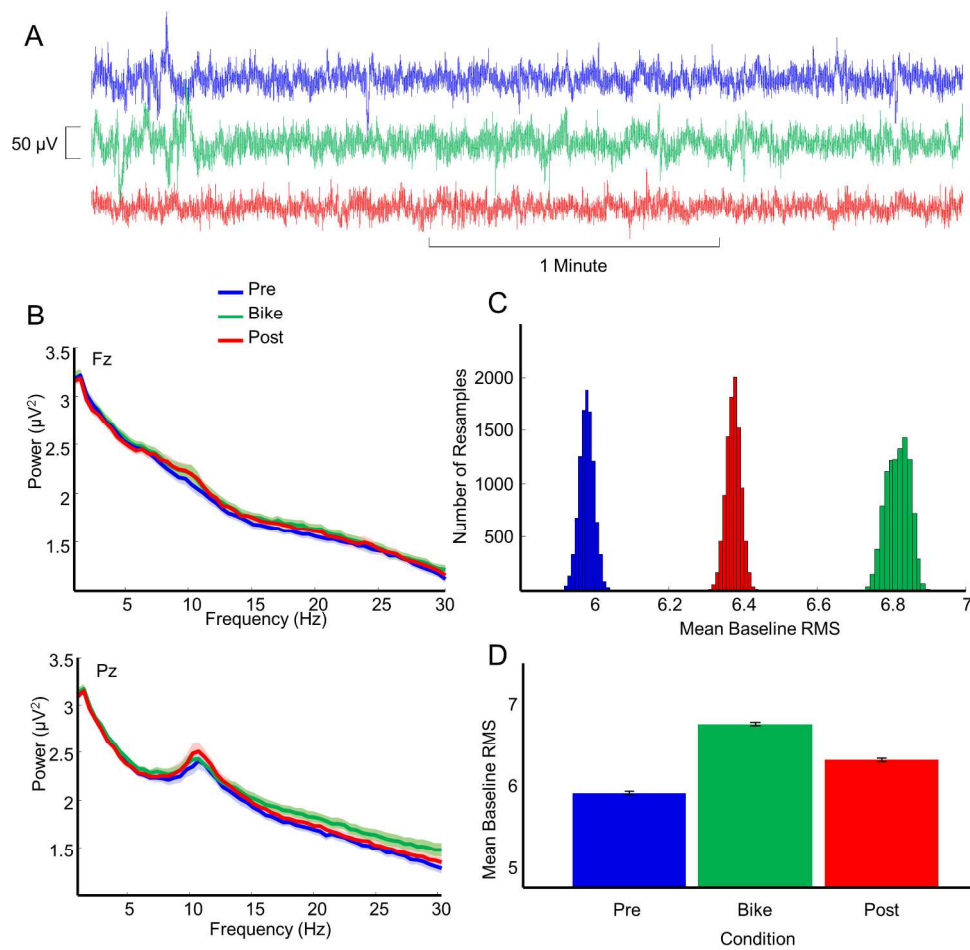


Figure 2. Single trial data noise levels. A: Raw EEG data (with notch filters and online bandpass) for a representative subject for several minutes in each of the pedaling conditions, shown at the Pz electrode location. B: Single-trial EEG spectra from electrodes Fz and Pz, computed with FFTs padded with zeros on 545 auditory target trial epochs of each subject, averaged over trials first, then subjects. Shaded regions indicate the standard error of the mean. C: Histogram of root mean square (RMS) grand average values collected during a 200ms baseline period, for 10,000 permutations of 300 randomly chosen standard target trials for each subject. RMS values are averaged over all electrodes within each trial, then averaged over trials, then subjects. D: Bar graph of these permuted distributions, with error bars representing standard deviation of the permuted distributions.

Figure 2
199x190mm (300 x 300 DPI)

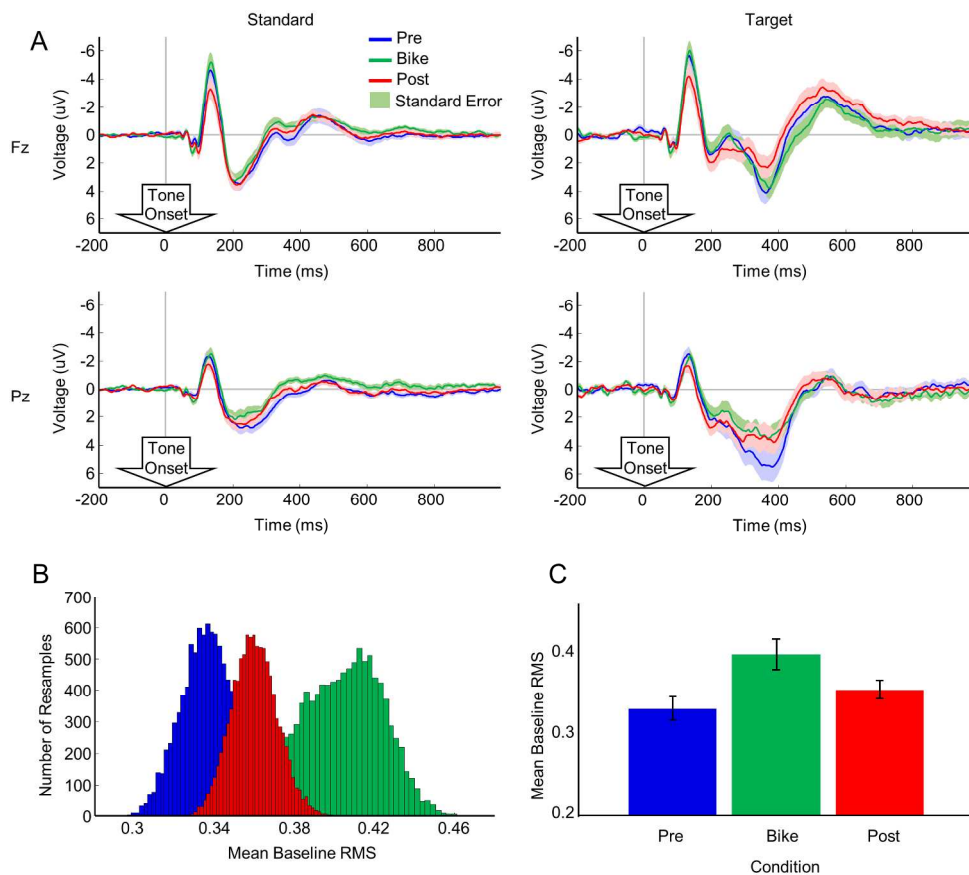


Figure 3. Baseline ERP noise. A: Grand average ERPs for the Fz and Pz electrodes, plotted separately to compare standards and targets between cycling conditions. Shaded areas represent the standard error of the mean. B: Histogram of ERP baseline RMS values, calculated using 10,000 randomly selected permutations of 300 target and standard trials for each subject. For each permutation, RMS of the baseline period is computed and the data are averaged over trials. C: Bar graph of these permuted distributions, with error bars representing standard deviation of the permuted distributions.

Figure 3
214x190mm (300 x 300 DPI)

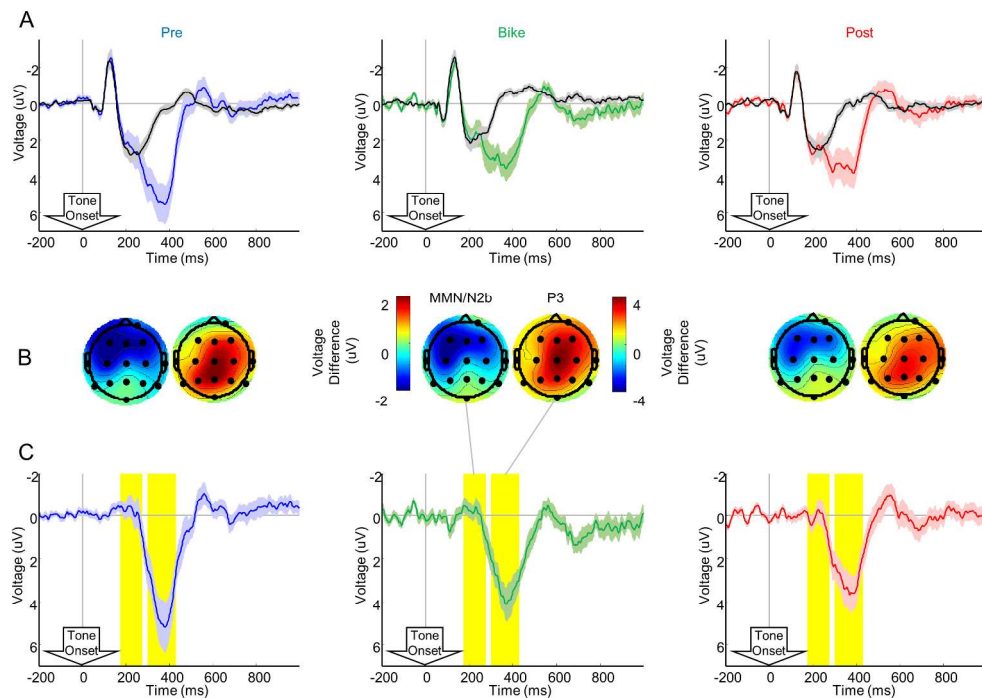


Figure 4. Event-related potential (ERP) grand averages. A: Grand average ERPs computed at electrode Pz for all artifact-free trials, corrected for eye movements, for both standard (black) and target (colour) tones. Positive is plotted down and shaded areas illustrate the standard error of the mean. B: Scalp topographies of the grand average ERP difference between standard and target tones in the MMN/N2b and P3 time-windows (indicated in yellow in 3C), 175-275ms and 300-430ms after the tone, respectively. EEG was re-referenced to the average of the left and right ear lobe electrodes. C: Difference wave ERPs from electrode Pz for each of the pedaling conditions, with shaded regions depicting within-subject standard error of the mean for this difference, having removed between-subject differences (Loftus and Masson, 1994). Regions highlighted in yellow depict the time-window for MMN/N2b and P3 analysis as well as topographic plotting.

Figure 4

254x181mm (300 x 300 DPI)

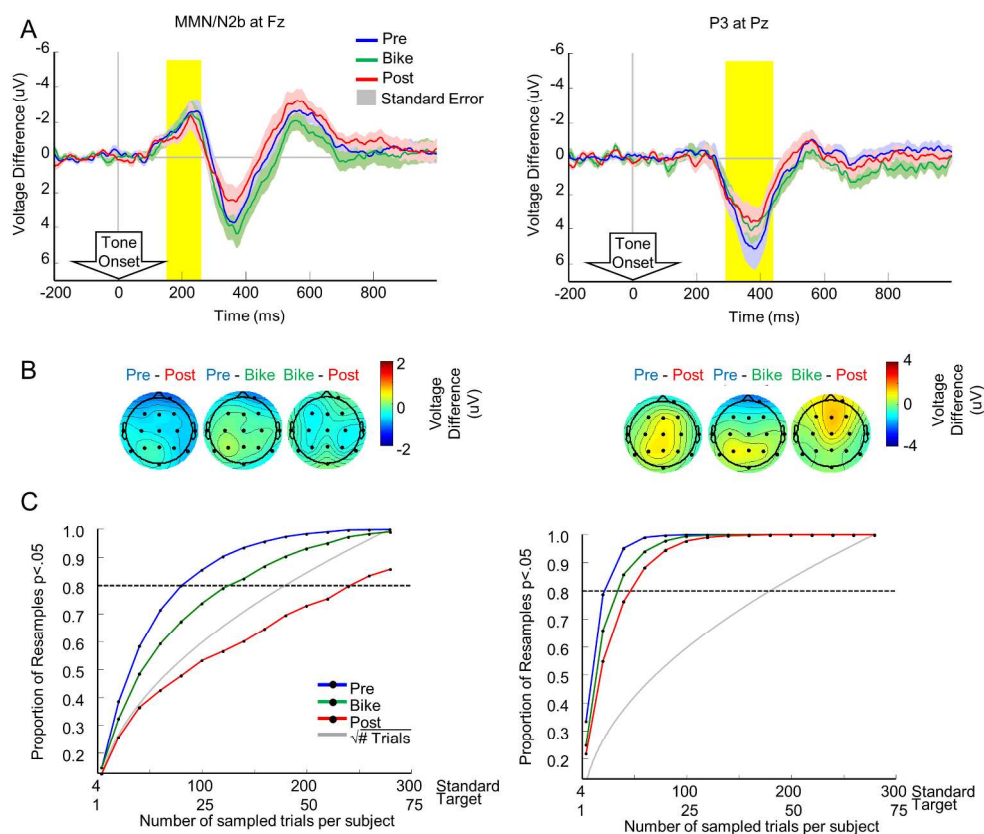


Figure 5. Difference waves and ERP power analysis. A: Difference waves depicting the average difference between standard and target trials for the three biking conditions are plotted for the Fz and Pz electrode locations. Yellow highlighted regions indicate the main time windows compared, namely the MMN/N2b at Fz (left) and the P3 at Pz (right). B: Topographies illustrating the voltage difference between conditions in the comparisons of the MMN/N2b at Fz and P3 at Pz (indicated in yellow regions of 5A) C: The results of a test of permutations in which a number of trials selected within 10,000 permutations varied between 5 and 280, while keeping the 4:1 ratio of standards to targets. Randomly selected trials are averaged to compute subject ERPs with each permutation for each number of trials. Before grand average statistics are computed, differences in the P3 and MMN/N2b time window between target and standard trials is calculated, and compared using an across subjects (paired-sample) one-tailed t-test ($\alpha = .05$). The graph plots the proportions of the 10,000 permutations for each number of trials in which an uncorrected significant difference obtained, for each of the cycling conditions. The dashed horizontal line at 0.8 represents the threshold to achieve 80% power to find an effect when one exists. The grey line shows a square root of the number of standard trials, scaled to a range between 0 and 1 on the vertical axis by dividing by the square root of the maximum number of trials.

Figure 5
224x190mm (300 x 300 DPI)